Calamity
Calamity: A Journal of Disaster Technology and Engineering
Calamity 3(2): 68–84
ISSN 3025-4140

Institute for Advanced Science, Social and Sustainable Future
MORALITY BEFORE KNOWLEDGE

# Spatial study of environmental vulnerability to earthquakes based on vegetation conditions

**Dionysius Otniel Santya Yudhistira**[1,*]
[1] *Urban and Regional Planning, Faculty of Science and Technology, Akademi Manajemen Informatika dan Komputer, Sleman, Special Region of Yogyakarta 55573, Indonesia.*
*Correspondence: nielsantya@gmail.com

Received Date: November 16, 2025 Revised Date: January 24, 2026 Accepted Date: January 29, 2026

## ABSTRACT

**Background:** Earthquakes are among the most destructive natural hazards, causing not only structural damage and loss of life but also long-term environmental degradation and vegetation decline. The ecological dimension of seismic vulnerability has often been overlooked in spatial studies, particularly in tropical regions. This research aims to assess environmental vulnerability to earthquakes based on vegetation conditions along the Opak Fault in the Special Region of Yogyakarta, Indonesia. **Methods:** The study employs a quantitative–spatial approach using Geographic Information Systems (GIS) to analyze vegetation coverage within three buffer zones at radii of 2 km, 5 km, and 10 km from the active fault line. Secondary data from the Geospatial Information Agency (BIG) and PVMBG were processed to calculate the Environmental Vulnerability Index (EVI) using the ratio of vegetated area to total buffer area, expressed as a percentage. **Findings:** Results indicate that vulnerability decreases with distance from the fault: 49% (high) for 0–2 km, 45% (high) for 2–5 km, and 40% (moderate) for 5–10 km. The innermost zones, dominated by irrigated rice fields on saturated alluvial soils, exhibit the highest susceptibility to liquefaction and ground shaking. In contrast, areas with greater forest cover show higher ecological resilience. **Conclusion:** The findings underscore the need to integrate vegetation-based management and Ecosystem-Based Disaster Risk Reduction (Eco-DRR) strategies into local spatial planning to strengthen environmental resilience in seismically active regions. **Novelty/Originality of this article:** This study uniquely combines GIS-based spatial analysis with vegetation data to assess earthquake vulnerability, highlighting ecological factors often overlooked in seismic risk assessments and informing ecosystem-based disaster risk reduction strategies.

**KEYWORDS**: active fault; environmental vulnerability; spatial analysis; vegetation.

## 1. Introduction

Earthquakes are among the most devastating geohazards worldwide, resulting in extensive human and ecological losses. Beyond the immediate physical destruction and casualties, seismic events often trigger cascading environmental impacts such as soil degradation, vegetation loss, and hydrological imbalance (UNDRR, 2023; Singh et al., 2022). These secondary consequences can persist long after the seismic shock, influencing landscape stability and ecological productivity. Globally, recent research trends have emphasized the importance of integrating environmental factors into disaster risk assessment to support more sustainable recovery strategies (UNEP, 2020; IUCN, 2021).

The Sendai Framework for Disaster Risk Reduction 2015–2030, adopted by the United Nations Office for Disaster Risk Reduction (UNDRR), highlights the need for ecosystem-based approaches to enhance disaster resilience. The framework calls for actions that

**Cite This Article:**
Yudhistira, D. O. S. (2026). Spatial study of environmental vulnerability to earthquakes based on vegetation conditions. *Calamity: A Journal of Disaster Technology and Engineering, 3*(2), 68–84. https://doi.org/10.61511/calamity.v3i2.2026.2559

protect, restore, and manage ecosystems as natural buffers against hazards. This concept, known as Ecosystem-Based Disaster Risk Reduction (Eco-DRR), underscores the dual role of ecosystems as both vulnerable elements and active agents in risk mitigation. Forests, vegetation, wetlands, and mangroves, for example, can absorb seismic shocks, stabilize soils, and minimize secondary hazards such as landslides and erosion (UNEP, 2020; FAO, 2020; IFRC, 2022).

According to the Ecosystem-Based DRR Guidelines by UNEP and the International Union for Conservation of Nature (IUCN), vegetation functions as a critical ecological infrastructure in hazard-prone landscapes. Dense root systems improve soil cohesion, canopy cover reduces raindrop impact and surface erosion, and vegetation density helps maintain hydrological balance after seismic disruption (IUCN, 2021). As a result, vegetation and land cover are increasingly recognized as key parameters in assessing environmental vulnerability, particularly in regions with high seismicity and intensive land-use changes.

In addition, the Post-Disaster Needs Assessment (PDNA) framework developed by FAO, UNDP, and the World Bank (2020) emphasizes vegetation recovery as a fundamental component of post-earthquake ecosystem rehabilitation. Healthy vegetation systems contribute to soil regeneration, biodiversity restoration, and reduction of secondary risks such as sedimentation and landslides. Similarly, the Green Response Framework introduced by the International Federation of Red Cross and Red Crescent Societies (IFRC, 2022) advocates for "green recovery" approaches, ensuring that disaster response efforts do not exacerbate environmental degradation. Together, these frameworks reflect a paradigm shift from purely physical reconstruction toward integrated ecological restoration.

Indonesia, located at the convergence of three major tectonic plates—Eurasian, Indo-Australian, and Pacific—experiences frequent seismic activity. The Meteorology, Climatology, and Geophysics Agency records thousands of earthquakes annually, many of which are shallow and potentially destructive (BMKG, 2024). The recurrence of such events highlights the urgency of incorporating environmental dimensions, particularly vegetation, into disaster risk assessments.

One of the most striking examples of the destructive potential of the Opak Fault is the 2006 Yogyakarta earthquake (Mw 6.3), which is widely associated with the reactivation of this fault system. The event resulted in more than 5,700 fatalities, over 150,000 damaged homes, and extensive modifications to the physical landscape, including liquefaction, ground ruptures, and widespread loss of vegetation cover (Hadiana et al., 2021; BMKG, 2024). Post-event assessments showed that the areas closest to the Opak Fault, particularly in Bantul and parts of Sleman, experienced the highest levels of structural and environmental damage due to the dominance of unconsolidated alluvial deposits and intensive agricultural land use. This disaster not only highlighted the seismic vulnerability of communities but also demonstrated the ecological fragility of landscapes intersected by active faults. The 2006 event therefore serves as a critical reference point for understanding how vegetation conditions interact with seismic hazard exposure, reinforcing the urgency of integrating ecological dimensions into earthquake vulnerability assessment in Yogyakarta.

The Special Region of Yogyakarta (DIY) is an exemplary area for this research due to its unique geological and ecological setting. The Opak Fault, a major active strike-slip fault extending from Prambanan to southern Bantul, is one of the most seismically active fault systems on the island of Java (Tidiesya et al., 2025; Ekarsti et al., 2023). The fault zone traverses a mosaic of land uses—paddy fields, mixed gardens, and settlements—situated predominantly on unconsolidated alluvial deposits. These geomorphological conditions make the region susceptible not only to ground shaking but also to secondary hazards such as liquefaction and soil instability.

Furthermore, the rapid expansion of urban areas and conversion of agricultural or vegetated lands into built-up zones exacerbate the environmental vulnerability. According to Jena et al. (2020), land-use transformation near active fault lines can significantly increase the exposure of human and ecological systems to seismic hazards. This issue is

particularly relevant in Bantul and Sleman Regencies, where the Opak Fault intersects highly productive yet environmentally fragile landscapes.

Previous studies conducted in Yogyakarta have mainly emphasized physical and social vulnerability assessments. Mardiatno et al. (2020) investigated multi-dimensional vulnerability at the village scale, focusing on infrastructure and socioeconomic indicators. However, only limited attention has been given to ecological or vegetation-based vulnerability, even though vegetation serves as both a stabilizing factor and an indicator of environmental recovery capacity (Andriani et al., 2023; Li et al., 2021). Studies from post-earthquake environments in Wenchuan and Sichuan, China, demonstrate that vegetation indices such as NDVI and land-cover heterogeneity can be used to measure the ecological resilience and recovery rate after seismic disturbances (Gan et al., 2019; Zhong et al., 2021; Liu et al., 2023).

Despite global recognition of Eco-DRR principles, there remains a significant research gap in Indonesia regarding the integration of vegetation conditions into earthquake vulnerability mapping. Most existing research adopts structural or geotechnical approaches, overlooking the ecological contributions of vegetation to environmental stability (Saputra et al., 2020; Wang et al., 2024). Moreover, quantitative evaluation of vegetation-related environmental vulnerability using spatial techniques remains scarce in Southeast Asia, where high population density and land-use intensity amplify disaster risks.

This gap underscores the need for comprehensive spatial analysis linking active fault proximity, vegetation distribution, and ecological vulnerability. The use of Geographic Information Systems (GIS) offers a reliable means to quantify spatial relationships between hazard sources and land-cover conditions, providing both visual and numerical insights into environmental risk (Goodchild, 2021; Wang et al., 2022).

In this context, the present study focuses on the spatial assessment of environmental vulnerability to earthquakes in Yogyakarta by analyzing vegetation conditions across buffer zones surrounding the Opak Fault. Three buffer radii—2 km, 5 km, and 10 km—were used to represent zones of high, medium, and low seismic exposure. The analysis aims to quantify the Environmental Vulnerability Index (EVI) for each zone and interpret the ecological implications of vegetation distribution relative to seismic hazards.

By combining spatial modelling with vegetation-based indicators, this study contributes to the development of evidence-based, ecosystem-oriented disaster management in Indonesia. The findings are expected to provide scientific input for sustainable spatial planning, vegetation restoration strategies, and policy integration under the Ecosystem-Based Disaster Risk Reduction (Eco-DRR) framework. Ultimately, the study seeks to strengthen the linkage between environmental conservation and disaster mitigation, particularly in fault-dominated landscapes such as the Opak Fault corridor in Yogyakarta.

## 2. Methods

### *2.1 Study area and approach*

This study was conducted in the Special Region of Yogyakarta (Daerah Istimewa Yogyakarta or DIY), which covers an area of approximately 3,186 km$^2$ and consists of five administrative regions: Sleman, Bantul, Gunungkidul, Kulonprogo, and Yogyakarta City. Geographically, DIY is located in the southern part of Java Island between latitudes 7°33′–8°12′ S and longitudes 110°02′–110°50′ E. The region lies in a tectonically active zone and is strongly influenced by the Opak Fault, a major strike-slip fault extending from Prambanan in the northeast to the southern coastal area of Bantul. This fault has generated several destructive earthquakes, including the 2006 Yogyakarta Earthquake (Mw 6.3), which caused severe structural and ecological impacts (BMKG, 2024; Ekarsti et al., 2023).

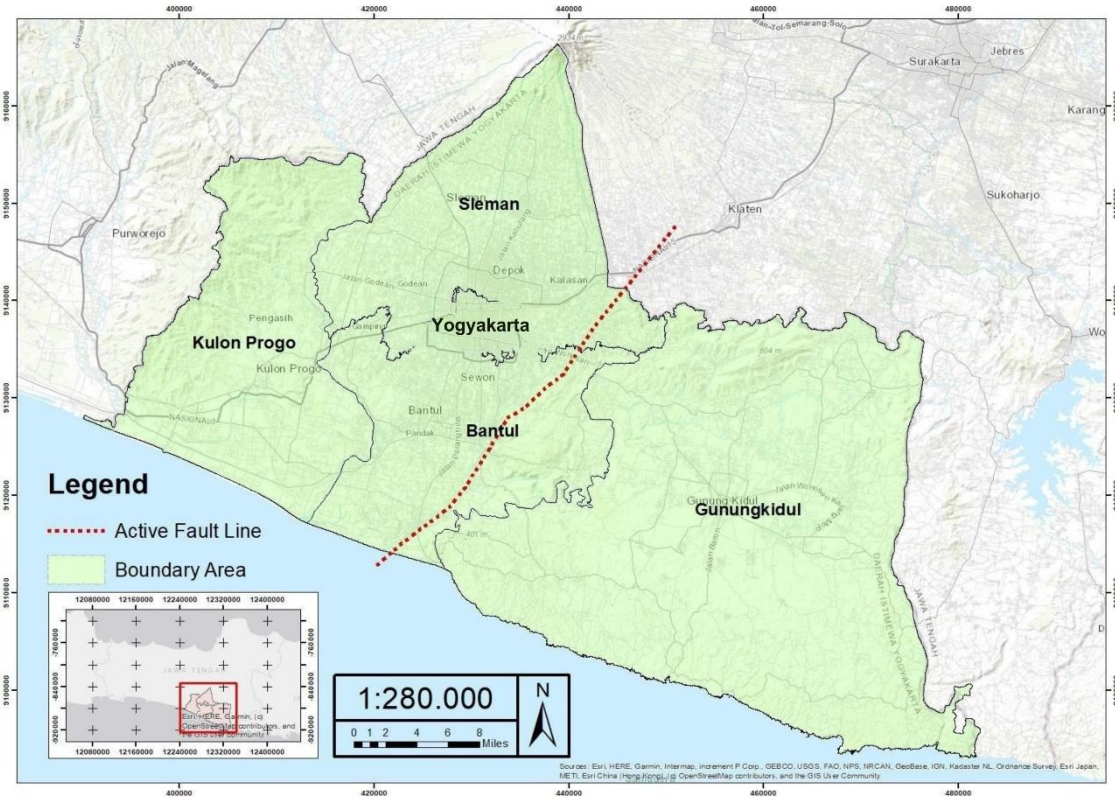


Fig. 1. Research location

The research adopted a quantitative–spatial approach using Geographic Information Systems (GIS) to assess vegetation-based environmental vulnerability. Spatial analysis techniques were applied to quantify the proportion and distribution of vegetated areas within three buffer distances from the Opak Fault. The analytical design allows for the identification of spatial correlations between seismic hazard exposure and the ecological capacity of the landscape. Although descriptive in interpretation, the analysis is grounded in measurable spatial and numerical data to ensure objectivity and reproducibility (Fotheringham et al., 2021; Wang et al., 2022).

Three buffer zones were defined at 2 km, 5 km, and 10 km distances from the Opak Fault line. These radii were chosen based on geophysical reasoning that surface deformation and amplification effects of shallow fault systems generally dissipate within a 10 km radius (Li et al., 2021; Zhong et al., 2021). The 0–2 km zone represents areas of highest exposure, the 2–5 km zone indicates moderate influence, and the 5–10 km zone reflects lower hazard intensity and transitional landscape stability.

Furthermore, the selection of the Special Region of Yogyakarta as the study area is supported by its representativeness as a complex socio-ecological system where tectonic activity, land-use dynamics, and population density interact intensively. The Opak Fault corridor intersects highly productive agricultural zones as well as rapidly urbanizing areas, making it an ideal case for examining the interaction between seismic hazard exposure and ecological vulnerability. This combination of geological sensitivity and anthropogenic pressure allows for a more comprehensive assessment of environmental vulnerability compared to regions with more homogeneous land-use patterns.

In addition, the quantitative–spatial approach employed in this study enables systematic comparison between different exposure zones by standardizing spatial units through buffer analysis. The use of concentric buffers not only simplifies the representation of hazard gradients but also facilitates reproducibility in similar studies conducted in other fault-controlled regions. This methodological framework ensures that variations in vegetation coverage can be directly attributed to differences in proximity to the fault, thereby strengthening the analytical validity of the results.

Moreover, the integration of GIS-based spatial analysis with environmental indicators enhances the robustness of the research design by allowing multi-layered data processing and spatial visualization. By combining geophysical parameters (distance from fault) with ecological variables (vegetation coverage), this approach provides a holistic perspective on environmental vulnerability. Such integration is essential in contemporary disaster studies, where single-factor analysis is often insufficient to capture the complexity of real-world hazard interactions.

### *2.2 Data and spatial processing*

The data used in this research consisted entirely of secondary datasets obtained from credible and official sources to ensure accuracy and spatial reliability. The primary dataset was the vegetation and land-use map in shapefile format provided by the Geospatial Information Agency/*Badan Informasi Geospasial*, which contains detailed classifications of land cover, including forest, mixed gardens, paddy fields, cropland, shrubs, and bare land. This dataset served as the foundation for identifying and quantifying vegetation distribution across the study area. In addition, the geometry of the active Opak Fault was extracted from the Center for Volcanology and Geological Hazard Mitigation/*Pusat Vulkanologi dan Mitigasi Bencana Geologi* (PVMBG) and verified using complementary data from the Lapak GIS repository to ensure positional accuracy of the fault trace. Supporting spatial layers, including topographic and administrative boundary maps, were also incorporated to maintain spatial alignment and cartographic consistency during analysis.

All datasets were standardized in the Universal Transverse Mercator (UTM) coordinate system Zone 49S (WGS 84) and harmonized at a working scale of 1:25,000, which is appropriate for provincial-level spatial analysis and ensures consistent spatial resolution. The spatial analysis was conducted using ArcGIS Desktop 10.8 through a sequence of geoprocessing operations, including buffer generation, spatial overlay, and area calculation. The initial stage involved generating concentric buffer zones at distances of 2 km, 5 km, and 10 km from the Opak Fault using the Buffer tool. These zones represent gradational levels of seismic influence, where areas closer to the fault are expected to experience stronger ground motion and higher deformation intensity.

The selection of these buffer distances was not arbitrary but grounded in both empirical observations and geophysical principles. Studies on fault avoidance and setback zones indicate that the impact of active faults extends beyond the rupture trace, requiring safety distances of several kilometers, particularly for critical infrastructure (He et al., 2022). Observations of co-seismic landslides and structural damage patterns further support the use of buffer distances in the range of 3–5 km to represent zones of significant hazard exposure. In addition, near-fault ground motion models for shallow crustal earthquakes demonstrate that seismic intensity is typically highest within the first 0–10 km from the fault before gradually attenuating with increasing distance (Bayless et al., 2019; Sedaghati et al., 2023). These findings justify the use of concentric buffers (2–5–10 km) to capture spatial variations in seismic influence.

Furthermore, recent studies on off-fault deformation reveal that structural and geomorphic impacts are not confined to the mapped fault line but extend laterally into surrounding areas. High-resolution analyses indicate that deformation zones may range from approximately 1 km up to 9 km in width, depending on fault maturity and tectonic conditions (Perrin et al., 2020; Zhao et al., 2023; Ding et al., 2024). This reinforces the conceptual basis that environmental vulnerability should be assessed within a broader spatial context rather than limited to the fault trace alone.

Following the buffer generation, spatial overlay analysis was conducted using the Intersect function in ArcGIS to combine the buffer zones with the vegetation land-use layer. This process enabled the identification and extraction of vegetation classes within each buffer zone, allowing for the calculation of vegetation area distribution. The Calculate Geometry function was subsequently used to quantify the total vegetated area ($Lv$) and the total area of each buffer zone ($Lt$). These values served as the primary inputs for computing

the Environmental Vulnerability Index (EVI), which represents the proportion of vegetation cover within each seismic exposure zone.

To ensure the validity and reliability of the spatial analysis, several verification procedures were performed. The fault geometry was cross-checked against official geological maps published by PVMBG, while vegetation classifications were validated using the latest BIG (2024) datasets and high-resolution satellite imagery. In addition, limited field verification was conducted at selected representative sites, including irrigated agricultural land in Bantul (0–2 km zone), mixed gardens in Sleman (2–5 km zone), and teak forest areas in Gunungkidul (5–10 km zone). These field observations confirmed a high degree of consistency between mapped data and actual vegetation conditions, thereby supporting the reliability of the GIS-based analytical framework applied in this study.

### *2.3 Environmental vulnerability index and classification*

The Environmental Vulnerability Index *(EVI)* was used to quantify the relationship between vegetation coverage and the level of environmental vulnerability in each buffer zone. The formula used in this study is as follows Equation 1, where *Lv* represents the total vegetated land area within each buffer zone measured in hectares, *Lt* denotes the total land area of the corresponding buffer zone in hectares, and *EVI* refers to the Environmental Vulnerability Index, which is expressed as a percentage (Trevisan et al., 2020; Coelho et al., 2024; Luo et al., 2024; Zou et al., 2017).

$$EVI = \frac{Lv}{Lt} \times 100 \quad \text{(Eq. 1)}$$

This formula measures the proportion of vegetation relative to the total area within each hazard buffer. A higher *EVI* value indicates greater vegetation coverage and consequently lower ecological vulnerability, while lower values denote higher environmental susceptibility due to limited vegetation protection and potential exposure to soil degradation, liquefaction, and erosion during seismic disturbances. To classify the degree of vulnerability, *EVI* values were grouped into five ordinal levels, adapted from Li et al. (2022), Zhou et al. (2023), and Wang & Yu (2025). The classification criteria are presented in Table 1.

Table 1. Ordinal classification of environmental vulnerability levels derived from the EVI

| EVI (%) | Vulnerability Level | Interpretation |
|---|---|---|
| >55% | Very High | Dense vegetation, low exposure to seismic degradation |
| 45–55% | High | Moderate vegetation, noticeable ecological stress |
| 35–44% | Moderate | Partial vegetation cover, transitional stability |
| 20–34% | Low | Sparse vegetation, increased susceptibility |
| <20% | Very Low | Bare or degraded areas, highly vulnerable |

The use of an ordinal classification simplifies comparison between zones while capturing ecological thresholds that distinguish stable from degraded environments. Ordinal scaling was selected because it effectively represents the nonlinear nature of ecological responses to disturbances (Li et al., 2022). The three computed EVI values—49% (2 km), 45% (5 km), and 40% (10 km)—correspond respectively to high, high, and moderate vulnerability levels. These classifications provide a basis for interpreting spatial variations in vegetation resilience relative to seismic influence. In interpreting the results, the EVI values were linked with geomorphological conditions and vegetation types across Yogyakarta. The 0–2 km buffer is largely composed of irrigated paddy fields on alluvial sediments, whereas outer zones contain mixed gardens and hilly forest areas. The index calculation thus captures how proximity to the active fault affects ecological vulnerability and landscape resilience.

## 3. Results and Discussion

### *3.1 Spatial distribution of vegetation and fault hazard zones*

The spatial overlay analysis revealed the distribution of vegetation types across the three buffer zones surrounding the Opak Fault. The active fault line extends in a northeast–southwest direction, passing through the districts of Sleman, Bantul, and Gunungkidul. The fault corridor cuts through various geomorphological units, from volcanic uplands in Sleman to alluvial plains in Bantul, and the limestone hills of Gunungkidul. These variations significantly affect the type and density of vegetation. The buffer analysis generated three zones representing different degrees of potential seismic influence—0–2 km (high hazard), 2–5 km (moderate hazard), and 5–10 km (low hazard). The resulting spatial configuration is presented in Figure 2, which illustrates the proximity of vegetation coverage relative to the active fault zone.

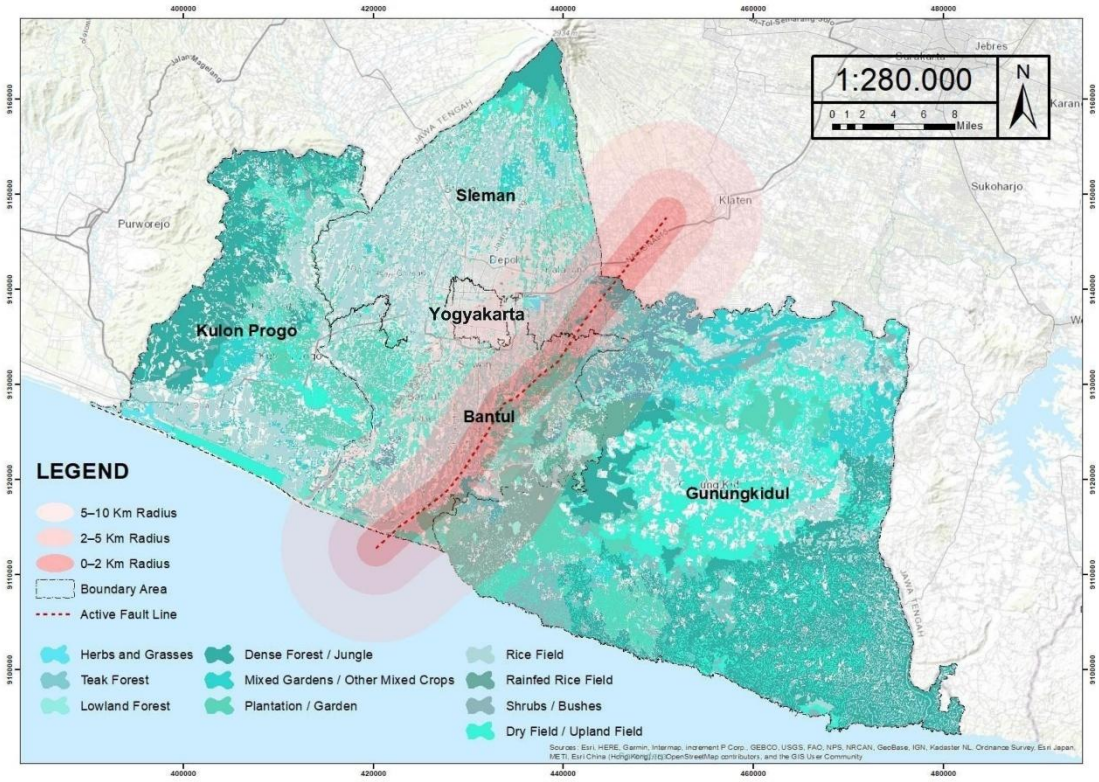


Fig. 2. Spatial Distribution of vegetation within the buffer zones

Figure 2 displays the spatial relationship between the Opak Fault and the vegetation cover across the Special Region of Yogyakarta, revealing a clear landscape mosaic shaped by geology, land use and human settlement. The fault trace cuts across distinct geomorphological units — volcanic uplands to the north, extensive alluvial plains through the central corridor, and karstic hills to the southeast — and this physiographic variation is reflected in the composition and continuity of vegetation. Vegetation patterns therefore do not follow a random distribution but are structured by underlying lithology, topography and longstanding patterns of agricultural use and urbanisation.

Visually, the mapped vegetation shows a gradient in both cover and structural complexity that broadly corresponds to distance from the fault corridor: areas adjacent to the fault tend to exhibit more fragmented and anthropogenic vegetation cover, while areas farther from the trace show larger, more contiguous patches of natural or semi-natural vegetation. This gradient is moderated by local relief and land-use history — for example, pockets of dense vegetation persist on steeper slopes and in karst uplands, whereas flat alluvial basins concentrated along the fault exhibit extensive cultivated land and

discontinuous natural cover. The figure therefore highlights a nested interplay between natural controls (soil, slope, lithology) and socio-economic drivers (agriculture, settlement) that together determine the ecological capacity of the landscape to absorb seismic disturbance.

From a hazard-vulnerability perspective, the map suggests heterogeneity in ecological resistance, contiguous forested patches and perennial plantations are spatially clustered in areas of more complex terrain and are likely to confer greater slope stability and hydrological regulation, whereas intensively managed croplands and built environments are predominant in the lowland corridors where soils are finer and water tables shallower. The juxtaposition of high-exposure linear fault geometry with expanses of human-modified land use therefore amplifies potential environmental impacts, because anthropogenic systems typically provide less root reinforcement and lower post-disturbance recovery potential than structurally diverse natural ecosystems.

It is also notable that administrative and infrastructural elements — settlements, roads and irrigation networks — are concentrated within and adjacent to segments of the fault corridor, increasing the socio-ecological exposure of these zones. The combined spatial patterns underscore that ecological vulnerability is not solely a function of vegetative area but is strongly conditioned by vegetation type, continuity and landscape context; hence, the map should be read as an integrative indicator of both exposure and ecological capacity rather than a simple proxy of risk.

Taken together, the mapped distribution provides an essential spatial framework for the subsequent buffer-based analyses (Sections 3.2–3.4). It identifies priority landscapes where vegetation restoration, conservation or land-use regulation could most effectively enhance ecological resilience to seismic events, and it visually justifies the decision to assess vulnerability using concentric buffers around the Opak Fault. The detailed, radius-specific results that follow will quantify these qualitative patterns and link them to policy-relevant recommendations.

A more detailed interpretation of Figure 2 further reveals the spatial dominance of specific vegetation types within each buffer zone. The innermost 0–2 km corridor is visually characterized by the prevalence of irrigated rice fields (sawah) and mixed agricultural land, particularly in Bantul and parts of Sleman. These land-use types appear as highly fragmented patches with relatively low structural complexity, indicating intensive human management and limited ecological buffering capacity. In contrast, the 2–5 km buffer begins to show increased heterogeneity, with a noticeable presence of mixed gardens (kebun campuran), plantations, and shrub vegetation that form transitional ecological patterns between lowland agriculture and upland vegetation systems.

In the outer 5–10 km buffer zone, the map highlights a more continuous distribution of forest-related land cover, including lowland forest, teak forest , and denser vegetation patches, particularly in Gunungkidul and parts of Kulon Progo. These areas exhibit higher vegetation continuity and structural diversity, which are important indicators of ecological stability. The visual contrast between the inner and outer buffers clearly demonstrates a spatial shift from anthropogenically dominated landscapes toward more natural or semi-natural ecosystems as the distance from the fault increases.

Additionally, the alignment of the fault trace with densely cultivated and populated areas—especially in the Bantul corridor—indicates a critical overlap between zones of high seismic exposure and high land-use intensity. This spatial coincidence significantly elevates environmental vulnerability, as areas with the highest hazard potential are also those with the least ecological resistance. The map thus not only illustrates vegetation distribution but also implicitly highlights priority zones for intervention, where vegetation reinforcement and land-use regulation are most urgently needed.

### *3.2 Vegetation distribution within the 0–2 km buffer zone*

The innermost 2 km buffer zone represents the area of highest environmental exposure to seismic activity along the Opak Fault. This zone is dominated by intensively

managed agricultural land, particularly in Bantul and Sleman Regencies, where flat alluvial plains support high productivity farming systems. Vegetation in this corridor consists primarily of shallow-rooted crops, limited patches of mixed gardens, and negligible forest cover, indicating a landscape heavily shaped by human use rather than natural ecological processes. The detailed distribution of vegetation types within this buffer zone is presented in Table 2.

Table 2. Distribution of vegetation land use within 2 km radius of the opak fault line

| | Bantul Regency | Sleman Regency | Gunungkidul Regency | Total (Ha) |
|---|---|---|---|---|
| Herbs and Grasses | 62.03 | 4.90 | - | 66.93 |
| Lowland Forest | 54.68 | - | - | 54.68 |
| Mixed Gardens/Other Mixed Crops | 327.66 | 717.45 | 15.93 | 1,061.04 |
| Plantation/Garden | 1,349.60 | 82.59 | 120.91 | 1.553.10 |
| Rice Field | 3,884.78 | 1,233.54 | 5.72 | 5,124.04 |
| Dry Field/Farmland | 1,843.76 | 47.16 | 1.96 | 1,892.87 |

As shown in Table 2, rice fields constitute the most dominant vegetation type, covering 5,124.04 ha, followed by plantation or garden crops (1,553.10 ha) and mixed gardens (1,061.04 ha). The total vegetated area in this buffer reaches 9,752.67 ha, equivalent to 49% of the total 2 km buffer area (20,031.07 ha). This highlights the predominance of agricultural land, with very limited representation of lowland forest (54.68 ha) and almost no shrubland or natural vegetation. The spatial pattern suggests a simplified vegetation structure dominated by shallow-rooted systems that offer limited capacity to reinforce soil and absorb ground vibrations.

The predominance of irrigated rice fields indicates that much of the core fault corridor lies on saturated alluvial deposits. Such soils are highly susceptible to liquefaction and differential settlement during seismic shaking, making the vegetation profile ecologically fragile. Areas in central Bantul—where rice fields cover extensive lowland surfaces—show the highest concentration of vulnerable vegetation conditions. Sleman contributes primarily mixed gardens and smaller rice field patches, whereas only marginal vegetation from Gunungkidul enters this radius due to the limited spatial intersection of the fault buffer with its limestone geomorphology.

Overall, the vegetation arrangement in this zone indicates high environmental vulnerability, consistent with its Environmental Vulnerability Index (EVI) score of 49%. The limited presence of deep-rooted vegetation such as forest or shrubland, combined with hydrologically unstable soils, results in minimal ecological buffering capacity. Consequently, the 0–2 km corridor represents the most environmentally fragile segment of the Opak Fault landscape.

A closer examination of the vegetation composition within this inner buffer also indicates a high degree of landscape homogenization, where agricultural monocultures dominate over ecologically diverse land-cover types. This condition reduces the functional resilience of the ecosystem, as uniform vegetation structures are generally less capable of withstanding and recovering from external disturbances compared to heterogeneous systems (Wang et al., 2022; Saputra et al., 2020). The limited variation in vegetation types within this zone further suggests that ecological processes such as nutrient cycling, soil stabilization, and water retention are heavily dependent on human management rather than natural regulation.

In addition, the spatial concentration of agricultural land in proximity to the fault line implies a potential compounding effect between seismic hazard and land-use intensity. Intensive farming practices, including frequent soil tillage and irrigation, may weaken soil structure over time, thereby increasing susceptibility to ground failure during seismic events. This interaction between anthropogenic land use and geophysical processes highlights the importance of incorporating sustainable land management practices into high-risk zones. Introducing vegetative buffers, contour planting, and reduced soil

disturbance techniques could help mitigate some of these risks by improving soil cohesion and reducing vulnerability to liquefaction.

Furthermore, the near absence of forested land within the 0–2 km buffer underscores a critical gap in ecological protection along the most hazard-prone segment of the fault corridor. Forest ecosystems typically provide stronger root reinforcement and greater surface stability, which are essential for minimizing secondary environmental impacts such as erosion and land subsidence. The lack of such vegetation in this zone indicates that ecological resilience is currently insufficient to counterbalance the high level of seismic exposure. Therefore, targeted ecological restoration efforts—particularly the introduction of deep-rooted vegetation systems—are necessary to enhance the environmental stability of this inner buffer zone.

### *3.3 Vegetation distribution within the 2–5 km buffer zone*

Expanding the analysis to the 2–5 km buffer zone reveals a more diverse vegetation composition compared to the innermost corridor. This transitional zone spans parts of Bantul, Sleman, Yogyakarta City, and the northern foothills of Gunungkidul, where agricultural landscapes gradually merge with mixed gardens and early forest regrowth. The vegetation patterns reflect both ecological and geomorphological transitions—shifting from lowland alluvial plains near the fault to more undulating terrain farther away. A detailed breakdown of vegetation types is presented in Table 3.

Table 3. Distribution of vegetation land use within 5 km radius of the opak fault line

| | Yogyakarta City | Bantul Regency | Sleman Regency | Gunungkidul Regency | Total (Ha) |
|---|---|---|---|---|---|
| Herbs and Grasses | - | 39.56 | 89.31 | 0.71 | 129.58 |
| Lowland Forest | - | 58.14 | - | - | 58.14 |
| Dense Forest/Jungle | - | 180.45 | - | - | 180.45 |
| Mixed Gardens/ Other Mixed Crops | - | 876.31 | 933.68 | 1,228 | 3,038 |
| Plantation/Garden | 2.27 | 1,627.13 | 190.54 | 951.11 | 2,771.05 |
| Rice Field | 0.01 | 4,808.47 | 1,809.63 | 368.11 | 6,986.23 |
| Shrubs/Bushes | - | 374.02 | 73.39 | 33.71 | 481.12 |
| Dry Field/Farmland | - | 1,598.82 | 117.89 | 144.54 | 1,861.26 |

As shown in Table 3, the total vegetated area in the 5 km buffer zone reaches 15,505.82 ha, representing 45% of the total buffer area (34,742.02 ha). Rice fields remain the dominant land cover type with 6,986.23 ha, but the presence of mixed gardens (3,038 ha) and plantations (2,771.05 ha) begins to increase significantly. Notably, this radius includes 180.45 ha of dense forest, marking the early appearance of more permanent vegetation structures not present in the 0–2 km zone. Shrubland (481.12 ha) also becomes more apparent, especially in transitional slopes of Sleman and Gunungkidul.

Compared to the core fault corridor, this zone exhibits a blend of cultivated and semi-natural vegetation. The increasing presence of perennial vegetation such as teak, fruit trees, and other mixed-crop systems enhances soil cohesion and supports hydrological stability. However, agricultural land—especially rice fields and plantations—still dominates more than half of the landscape, indicating that ecological resilience remains moderate. Areas around central Bantul and western Sleman continue to rely heavily on monoculture crop systems, which contribute to landscape fragmentation and reduced structural vegetation complexity.

The Environmental Vulnerability Index (EVI) for this zone is 45%, placing it within the high vulnerability category. Although ecological conditions improve compared to the 0–2 km radius, the combination of human-modified land use, partially saturated soils, and fragmented vegetation results in a landscape that retains considerable susceptibility to seismic disturbances. This zone represents a transitional ecological buffer but has not yet developed sufficient structural vegetation to substantially decrease vulnerability.

A more detailed assessment of this intermediate buffer zone highlights its role as a critical transition area where both vulnerability and resilience factors coexist. The coexistence of agricultural land and semi-natural vegetation creates a heterogeneous landscape structure that can either enhance or weaken ecological stability depending on spatial configuration and management practices. Fragmented patches of mixed gardens and shrubs, although contributing to biodiversity, may not yet form sufficiently connected ecological networks to provide effective landscape-scale buffering against seismic disturbances (Wang et al., 2022; Zhong et al., 2021). This indicates that the current vegetation pattern, while more diverse than the inner buffer, still lacks the structural continuity required for optimal resilience.

Moreover, the spatial distribution of vegetation in this zone suggests the influence of topographic variation on land-use patterns. Areas with slightly higher elevation or sloping terrain—particularly toward Gunungkidul—tend to support more perennial vegetation such as mixed gardens and plantations, whereas flatter areas in Bantul and Sleman remain dominated by irrigated rice fields. This differentiation reinforces the idea that geomorphological conditions play a key role in shaping both vegetation distribution and environmental vulnerability. Consequently, integrating topography-based land-use planning could enhance the effectiveness of vegetation management strategies in reducing seismic risk.

From a management perspective, this buffer zone presents significant opportunities for ecological intervention. Strengthening vegetation connectivity through reforestation corridors, agroforestry expansion, and the protection of existing shrub and forest patches could substantially improve ecological resilience. Unlike the inner 0–2 km zone, where structural constraints are more pronounced, the 2–5 km zone offers greater flexibility for implementing landscape-scale ecological improvements. Therefore, targeted interventions in this transitional zone could serve as a strategic approach to gradually reduce vulnerability while maintaining economic productivity.

### *3.4 Vegetation distribution within the 5–10 km buffer zone*

The 5–10 km buffer zone covers the broadest ecological variation, spanning upland volcanic areas in Sleman, limestone hills in Gunungkidul, and parts of the Kulonprogo foothills. This outer radius marks a pronounced transition from intensively managed agricultural land toward more natural vegetation formations, including forests, dense mixed gardens, and upland plantations. The distribution of vegetation types within this buffer zone is detailed in Table 4.

Table 4. Distribution of vegetation land use within 10 km radius of the opak fault line

| | Yogyakarta City | Bantul Regency | Sleman Regency | Gunungkidul Regency | Kulonprogo Regency | Total (Ha) |
|---|---|---|---|---|---|---|
| Herbs and Grasses | 30.77 | - | 149.88 | - | - | 180.65 |
| Lowland Forest | - | 1,179.31 | - | 1,192.80 | - | 2,372.11 |
| Dense Forest/ Jungle | - | 1,179.31 | - | 1,192.80 | - | 2,372.11 |
| Mixed Gardens /Other Mixed Crops | - | 1,044.60 | 400.29 | 3,877.99 | 65.06 | 5,322.87 |
| Plantation/ Garden | 17.40 | 1,786.48 | 577.26 | 4,697.13 | 62.27 | 7,078.26 |
| Rice Field | 27.59 | 4,439.37 | 2,396.92 | 1,437.04 | 241.08 | 8,300.93 |
| Shrubs/ Bushes | - | 274.81 | 7.07 | 186.89 | 164.28 | 468.78 |
| Dry Field/ Farmland | 11.03 | 1,324.08 | 250.47 | 700.90 | 66.60 | 2,286.49 |

As presented in Table 4, the 5–10 km buffer zone contains the highest total vegetated area—28,382.2 ha, equivalent to 40% of the total buffer area (70,423.37 ha). This zone is characterised by substantial forest cover, with lowland forest reaching 2,372.11 ha and dense mixed vegetation covering 5,322.87 ha. Plantation land (7,078.26 ha) and rice fields (8,300.93 ha) remain present but are more dispersed and integrated into hilly terrain. Shrubland (468.78 ha) and dryland farming (2,286.49 ha) also exhibit increased spatial coverage, particularly in Gunungkidul's karst landscapes.

The vegetation profile in this outer zone indicates a more ecologically stable landscape. Extensive forest cover, combined with perennial crops and mixed vegetation mosaics, reinforces soil structure and provides natural buffering against seismic-induced disturbances. The presence of rugged topography—especially in Gunungkidul's limestone hills—further enhances ecological resilience by reducing susceptibility to liquefaction and ground settlement. However, certain lowland pockets in Bantul and Sleman still exhibit concentrated rice fields, indicating localized vulnerability despite the broader trend of increased vegetation complexity.

Overall, the 5–10 km buffer zone demonstrates moderate environmental vulnerability, reflected in its EVI score of 40%. Although it contains the most extensive vegetation area and the highest proportion of forested land, the presence of agricultural clusters and mixed land uses prevents the zone from achieving a low vulnerability rating. Nevertheless, ecological stability in this zone is markedly higher than the inner buffers, reaffirming the gradient of vulnerability that decreases with greater distance from the Opak Fault.

A further interpretation of this outer buffer zone emphasizes the importance of vegetation continuity and structural complexity in enhancing ecological resilience. Unlike the inner and intermediate buffers, vegetation in the 5–10 km zone tends to form larger and more contiguous patches, particularly in forested and mixed-vegetation areas. This spatial continuity allows ecological processes—such as nutrient cycling, water infiltration, and root reinforcement—to operate more effectively at the landscape scale, thereby increasing the system's capacity to absorb and recover from seismic disturbances (Wang et al., 2022; Li et al., 2021). As a result, this zone functions as a natural ecological buffer that can mitigate the propagation of secondary environmental impacts originating from the fault corridor.

In addition, the influence of geomorphological heterogeneity is more pronounced in this buffer zone. The presence of karst landscapes in Gunungkidul and volcanic uplands in Sleman creates varied soil conditions and slope gradients that support diverse vegetation types. These physical characteristics not only promote biodiversity but also reduce uniform vulnerability across the landscape. Areas with steeper slopes and well-established vegetation tend to exhibit higher resistance to ground deformation, whereas flatter lowland pockets remain more susceptible due to finer soil textures and higher groundwater levels. This spatial variability highlights the need for localized assessments within broader buffer zones.

From a spatial planning perspective, the 5–10 km buffer zone holds significant potential as a priority area for conservation and ecosystem-based disaster risk reduction (Eco-DRR). Maintaining existing forest cover and preventing further land conversion are critical to preserving the ecological functions that contribute to hazard mitigation. Additionally, reinforcing connections between forest patches through ecological corridors could further enhance landscape resilience and support long-term environmental stability. Strategic management in this zone would not only reduce seismic vulnerability but also provide co-benefits such as biodiversity conservation, carbon storage, and sustainable land use.

### *3.5 Discussion: Spatial gradient and Eco-DRR implications*

The results highlight a consistent inverse relationship between distance from the fault and environmental vulnerability. The Environmental Vulnerability Index (EVI) decreases from 49% in the 0–2 km zone to 45% in the 2–5 km zone, and 40% in the 5–10 km zone. This declining trend reflects an improvement in vegetation coverage and ecosystem

stability with increasing distance from the fault. However, the vulnerability in the core and intermediate zones remains high due to intensive agricultural activity and limited vegetation diversity.

From an Eco-DRR perspective, these findings underscore the critical role of vegetation management in reducing seismic risk. In the immediate 2 km corridor, introducing riparian buffers, deep-rooted vegetative strips, and perennial agroforestry systems could enhance soil cohesion and reduce liquefaction susceptibility. In the 2–5 km zone, promoting mixed cropping systems and vegetation restoration in degraded plots could strengthen ecological connectivity. Meanwhile, the outer 5–10 km zone serves as a potential ecological buffer belt, where forest conservation and reforestation efforts should be prioritized to maintain slope stability and hydrological balance.

Integrating vegetation-based vulnerability assessments into regional spatial planning (RTRW) is essential for aligning land-use practices with seismic risk reduction. The EVI framework provides a simple yet evidence-based metric for identifying priority areas for ecological rehabilitation. By incorporating such indices into spatial zoning regulations, policymakers can enhance landscape resilience while maintaining agricultural productivity. These recommendations align with global best practices outlined in the UNDRR's Sendai Framework (2015–2030) and the UNEP Eco-DRR Guidelines (2020), which advocate the use of ecosystem-based solutions for disaster mitigation and recovery.

Beyond the observed spatial gradient, the findings also highlight the importance of considering multi-scalar interactions between ecological conditions and seismic processes. Environmental vulnerability in fault-dominated landscapes is not solely determined by proximity to the hazard source but is also shaped by land-use intensity, vegetation structure, and geomorphological context. This suggests that vulnerability is inherently dynamic and context-dependent, requiring integrated assessment approaches that combine physical, ecological, and socio-economic variables. The present study, by focusing on vegetation as a key ecological indicator, contributes to bridging this gap, although future research could further refine the model by incorporating additional parameters such as soil characteristics, groundwater conditions, and land-use change dynamics.

In addition, the concept of ecological resilience emerging from this study reinforces the relevance of landscape-based approaches in disaster risk reduction. Rather than treating vegetation merely as a passive land-cover component, it should be understood as an active system that can mitigate hazard impacts and facilitate post-disaster recovery. The variation in EVI values across buffer zones demonstrates how ecosystem structure and function influence the capacity of landscapes to absorb disturbances. This insight aligns with recent advances in resilience theory, which emphasize the role of diversity, redundancy, and connectivity in maintaining system stability under stress.

Furthermore, the application of the Environmental Vulnerability Index (EVI) as a spatial indicator offers practical implications for policy and planning. Its simplicity allows for easy integration into existing spatial decision-support systems, while its ecological basis ensures that environmental considerations are not overlooked in hazard mitigation strategies. However, it is important to acknowledge that the EVI, as applied in this study, primarily captures vegetation quantity rather than quality or functional characteristics. Future methodological improvements could incorporate vegetation health indices (e.g., NDVI), species composition, and ecosystem services valuation to provide a more comprehensive assessment of ecological vulnerability.

## 4. Conclusions

This study assessed the environmental vulnerability of the Opak Fault corridor in Yogyakarta by analysing the distribution and composition of vegetation across three buffer zones (0–2 km, 2–5 km, and 5–10 km). The spatial analysis revealed a clear gradient of ecological vulnerability that decreases with increasing distance from the active fault line. The innermost zone (2 km radius) is dominated by irrigated rice fields and highly modified agricultural land situated on saturated alluvial deposits, resulting in the highest

Environmental Vulnerability Index (EVI) of 49%. The intermediate zone (2–5 km) shows a more diverse vegetation structure, yet agricultural land remains dominant, contributing to a high EVI of 45%. The outermost zone (5–10 km) contains the largest extent of forested and mixed perennial vegetation, producing a moderate EVI of 40%.

The vegetation patterns across the buffer zones demonstrate that ecological vulnerability in active fault landscapes is strongly shaped by land-use intensity and vegetation structure. Areas with simplified, shallow-rooted vegetation such as rice fields and monoculture plantations exhibit lower soil reinforcement and reduced ecological resilience, making them more susceptible to liquefaction, erosion, and seismic amplification. In contrast, zones with deeper-rooted forest vegetation and mixed agroforestry systems provide greater slope stability, improved hydrological regulation, and stronger resistance to seismic disturbance. These findings align with recent Eco-DRR literature, reaffirming that vegetation plays a critical role as both an indicator and a determinant of environmental vulnerability.

From a policy perspective, the results underscore the necessity of integrating vegetation-based vulnerability assessment into disaster risk reduction and spatial planning efforts in Yogyakarta. The presence of the Opak Fault within densely cultivated agricultural corridors highlights the urgent need for strengthening protection measures within fault-proximal zones, including the implementation of structural setback zones, vegetation restoration programs, and agroforestry-based land management. Additionally, the findings support the mandates of regional spatial planning regulations (RTRW), particularly those governing geological protected areas, by providing empirical justification for conservation, rehabilitation, and controlled land use around the Opak Fault.

Future research should incorporate more detailed geotechnical parameters—such as soil density, groundwater depth, and lithological profiles—to complement vegetation-based vulnerability mapping. Integrating satellite-derived vegetation indices, temporal land-use change analysis, and socio-economic exposure datasets would further enhance the accuracy of environmental vulnerability models. Such advancements will contribute to evidence-driven strategies for ecosystem-based disaster risk reduction, enabling Yogyakarta to develop more resilient landscapes that are capable of withstanding future seismic events.

## Acknowledgement

The author would like to express sincere gratitude to the lecturers and academic supervisors from the Urban and Regional Planning Department, Faculty of Science and Technology, Universitas Amikom Yogyakarta, for their guidance throughout the research process. Appreciation is also extended to the Badan Informasi Geospasial (BIG) and BMKG for providing essential spatial and seismic data that supported this study. The author acknowledges the support of colleagues who contributed feedback, technical assistance, and encouragement during the preparation of this manuscript.

## Author Contribution

All components of this research—including conceptualization, methodology, data processing, GIS analysis, validation, formal analysis, investigation, data curation, writing (original draft and revisions), visualization, and project administration—were carried out independently by D.O.S.Y. as the sole author.

## Funding

This research received no external funding

## Ethical Review Board Statement

Not available.

## Informed Consent Statement

Not available.

## Data Availability Statement
Not available.

## Conflicts of Interest
The author declare no conflict of interest.

## Declaration of Generative AI Use
The author used OpenAI's GPT tools only for minor language refinement and formatting assistance. All research ideas, analyses, and conclusions are fully the author's own, and all AI-assisted outputs were independently reviewed for accuracy and integrity.

## Open Access


## References
Andriani, R., Saputra, E., & Wibowo, A. (2023). Environmental degradation following the 2006 Yogyakarta earthquake: Impacts on vegetation and soil stability. *Environmental Earth Sciences, 82*(6), 301. https://doi.org/10.1007/s12665-023-10831-7

Bayless, J., & Abrahamson, N. (2019). Summary of the BA18 ground-motion model for Fourier amplitude spectra for crustal earthquakes in California. *Bulletin of the Seismological Society of America, 5,* 2088-2105. https://doi.org/10.1785/0120190077

BMKG. (2024). *Seismic activity and fault mapping in Java Island, Indonesia*. Badan Meteorologi, Klimatologi, dan Geofisika.

Coelho, C., Da Silva, D., Amorim, R., Vasconcelos, B., Possato, E., Filho, E., Brandão, P., Neto, J., & Silva, L. (2024). Development and application of an Environmental Vulnerability Index (EVI) for identifying priority restoration areas in the São Francisco River Basin, Brazil. *Land, 13*(9), 1475. https://doi.org/10.3390/land13091475

Ding, C., Dong, J., Béon, M., Lee, C., Ho, S., & Wang, S. (2024). Characterization of the active fault deformation zone of the Chegualin Fault in the alluvial plain of southwestern Taiwan. *Engineering Geology, 342,* 107740. https://doi.org/10.1016/j.enggeo.2024.107740

Dorn, H., Törnros, T., & Zipf, A. (2015). Quality evaluation of VGI using authoritative data: A comparison with land use data in southern Germany. *ISPRS International Journal of Geo-Information, 4*, 1657–1671. https://doi.org/10.3390/ijgi4031657

Ekarsti, L. D., Hadiana, R., & Setiadi, M. (2023). Mapping seismic vulnerability zones of the Opak Fault, Yogyakarta, using microtremor analysis and GIS. *Journal of Asian Earth Sciences, 252*, 106485. https://doi.org/10.1016/j.jseaes.2023.106485

FAO. (2020). *Restoration guidelines for ecosystem recovery after natural disasters*. Food and Agriculture Organization.

Fotheringham, A. S., Brunsdon, C., & Charlton, M. (2021). *Quantitative geography: Spatial analysis and GIS applications*. Sage Publications.

Gan, W., Liu, X., & Zhong, L. (2019). Vegetation recovery after the 2008 Wenchuan earthquake: A decadal perspective. *Remote Sensing of Environment, 235*, 111444. https://doi.org/10.1016/j.rse.2019.111444

Giuliani, G., Rodila, D., Külling, N., Maggini, R., & Lehmann, A. (2022). Downscaling Switzerland land use/land cover data using nearest neighbors and an expert system. *Land, 11*(5), 615. https://doi.org/10.3390/land11050615

Goodchild, M. F. (2021). Spatial data accuracy and uncertainty in environmental modelling. *International Journal of Geographical Information Science, 35*(9), 1735–1752. https://doi.org/10.1080/13658816.2021.1897642

Hadiana, R., Ekaristi, L. D., & Masykuri, M. (2021). Seismic hazard and liquefaction potential in Yogyakarta: Integrating soil and fault line mapping. *Geotechnical and Geological Engineering, 39*, 5483–5502. https://doi.org/10.1007/s10706-021-01751-1

He, X., Xu, C., Xu, X., & Yang, Y. (2022). Advances on the avoidance zone and buffer zone of active faults. *Natural Hazards Research*. https://doi.org/10.1016/j.nhres.2022.05.001

IFRC. (2022). *Green response quick guide: Environmentally sustainable disaster response*. International Federation of Red Cross and Red Crescent Societies.

IUCN. (2021). *Guidelines for ecosystem-based disaster risk reduction and climate change adaptation*. International Union for Conservation of Nature.

Jena, R., Pradhan, B., & Homaifar, A. (2020). Spatial multi-hazard vulnerability assessment using GIS and machine learning. *Sustainability, 12*(9), 3676. https://doi.org/10.3390/su12093676

Li, D., Chen, W., & Sun, H. (2021). Quantifying vegetation contribution to seismic ecological resilience in fault-affected regions. *Ecological Indicators, 131*, 108192. https://doi.org/10.1016/j.ecolind.2021.108192

Li, J., Zhang, H., & Xu, Q. (2022). Ordinal classification of environmental vulnerability in seismically active mountain regions. *Environmental Monitoring and Assessment, 194*(10), 667. https://doi.org/10.1007/s10661-022-10302-4

Liu, P., Pei, J., Guo, H., Tian, H., Fang, H., & Wang, L. (2022). Evaluating the accuracy and spatial agreement of five global land cover datasets in the ecologically vulnerable South China karst. *Remote Sensing, 14*, 3090. https://doi.org/10.3390/rs14133090

Liu, Z., Gan, W., & Zhong, L. (2023). Ten years of vegetation recovery after the Wenchuan earthquake: A multi-sensor analysis. *Remote Sensing, 15*(3), 655. https://doi.org/10.3390/rs15030655

Luo, M., Jia, X., Zhao, Y., Zhang, P., & Zhao, M. (2024). Ecological vulnerability assessment and its driving force based on ecological zoning in the Loess Plateau, China. *Ecological Indicators, 159,* 111658. https://doi.org/10.1016/j.ecolind.2024.111658

Mardiatno, D., Handayani, T., Susanto, D., Faida, L. R., Kusumasari, B., & Malawani, M. N. (2020). Earthquake vulnerability mapping in the at-risk Opak fault, Sengon village, Central Java, Indonesia. *E3S Web of Conferences, 200*, 01002. https://doi.org/10.1051/e3sconf/202020001002

Perrin, C., Waldhauser, F., & Scholz, C. (2020). The shear deformation zone and the smoothing of faults with displacement. *Journal of Geophysical Research: Solid Earth, 126*. https://doi.org/10.1029/2020JB020447

Phiri, D., Simwanda, M., Salekin, S., Nyirenda, V., Murayama, Y., & Ranagalage, M. (2020). Sentinel-2 data for land cover/use mapping: A review. *Remote Sensing, 12*, 2291. https://doi.org/10.3390/rs12142291

PVMBG. (2023). *Peta sesar aktif Indonesia*. Pusat Vulkanologi dan Mitigasi Bencana Geologi.

Saputra, E., Wibowo, A., & Andriani, R. (2020). Integrating vegetation dynamics and seismic hazard mapping for environmental risk assessment. *Natural Hazards, 104*(3), 2575–2593. https://doi.org/10.1007/s11069-020-04250-6

Sedaghati, F., & Pezeshk, S. (2023). Machine learning–based ground motion models for shallow crustal earthquakes in active tectonic regions. *Earthquake Spectra, 39*, 2406–2435. https://doi.org/10.1177/87552930231191759

Singh, R., & Kumar, D. (2022). Global review of vegetation response to earthquakes: Mechanisms and monitoring perspectives. *Progress in Earth and Planetary Science, 9*, 14. https://doi.org/10.1186/s40645-022-00477-5

Trevisan, D., Bispo, P., Almeida, D., Imani, M., Balzter, H., & Moschini, L. (2020). Environmental vulnerability index: An evaluation of water and vegetation quality in a

Brazilian savanna and seasonal forest biome. *Ecological Indicators, 112*, 106163. https://doi.org/10.1016/j.ecolind.2020.106163

UNDRR. (2015). *Sendai framework for disaster risk reduction 2015–2030*. United Nations Office for Disaster Risk Reduction. https://www.undrr.org/publication/sendai-framework-disaster-risk-reduction-2015-2030

UNDRR. (2023). *Global assessment report on disaster risk reduction 2023: Our world at risk*. United Nations Office for Disaster Risk Reduction. https://www.undrr.org/gar

UNEP. (2020). *Ecosystem-based approaches to disaster risk reduction: Implementing nature-based solutions*. United Nations Environment Programme.

Wang, H., Yan, H., Hu, Y., Xi, Y., & Yang, Y. (2022). Consistency and accuracy of four high-resolution LULC datasets: Indochina Peninsula case study. *Land, 11*(5), 758 https://doi.org/10.3390/land11050758

Wang, J., Zhang, Y., & Huang, Q. (2024). GIS-based environmental vulnerability mapping in seismically active regions. *International Journal of Applied Earth Observation and Geoinformation, 127*, 103602. https://doi.org/10.1016/j.jag.2024.103602

Wang, S., Li, J., & Zhou, X. (2022). Spatial modelling of vegetation-based environmental resilience to earthquakes. *Ecological Modelling, 471*, 110008. https://doi.org/10.1016/j.ecolmodel.2022.110008

World Bank. (2020). *Forest restoration following earthquake damage*. World Bank. https://openknowledge.worldbank.org/bitstreams/8c320cbc-1c7f-5c93-bb50-efac712da17d/download

Zhao, D., Qu, C., Bürgmann, R., & Shan, X. (2023). Characterizing deep, shallow, and surface fault zone deformation of the 2021 Mw 7.4 Maduo earthquake. *Seismological Research Letters, 95*(1), 277–287. https://doi.org/10.1785/0220230115

Zhong, L., Gan, W., & Liu, Z. (2021). Post-earthquake vegetation succession as an indicator of ecosystem resilience. *Ecological Indicators, 129*, 107924. https://doi.org/10.1016/j.ecolind.2021.107924

Zhou, X., Li, J., & Wang, D. (2023). Quantitative classification of environmental vulnerability based on vegetation index and fault proximity. *Sustainability, 15*(3), 2121. https://doi.org/10.3390/su15032121

Zou, T., & Yoshino, K. (2017). Environmental vulnerability evaluation using a spatial principal components approach in the Daxing'anling region, China. *Ecological Indicators, 78*, 405–415. https://doi.org/10.1016/j.ecolind.2017.03.039

## Biography of Author

**Dionysius Otniel Santya Yudhistira,** Urban and Regional Planning, Faculty of Science and Technology, Akademi Manajemen Informatika dan Komputer, Sleman, Special Region of Yogyakarta 55573, Indonesia.

- Email: nielsantya@gmail.com
- ORCID: 0009-0004-5736-7425
- Web of Science ResearcherID: N/A
- Scopus Author ID: N/A
- Homepage: N/A